



Graphdiyne as a high-capacity lithium ion battery anode material

Byungryul Jang, Jahyun Koo, Minwoo Park, Hosik Lee, Jaewook Nam, Yongkyung Kwon, and Hoonkyung Lee

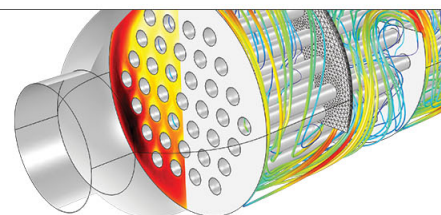
Citation: [Applied Physics Letters](#) **103**, 263904 (2013); doi: 10.1063/1.4850236

View online: <http://dx.doi.org/10.1063/1.4850236>

View Table of Contents: <http://scitation.aip.org/content/aip/journal/apl/103/26?ver=pdfcov>

Published by the [AIP Publishing](#)

Over **700** papers &
presentations on
multiphysics simulation



VIEW NOW ►

 COMSOL

Graphdiyne as a high-capacity lithium ion battery anode material

Byungryul Jang,¹ Jahyun Koo,¹ Minwoo Park,¹ Hosik Lee,² Jaewook Nam,³
 Yongkyung Kwon,¹ and Hoonkyung Lee^{1,a)}

¹School of Physics, Konkuk University, Seoul 143-701, South Korea

²School of Mechanical and Advanced Materials Engineering, Ulsan National Institute of Science and Technology (UNIST), Ulsan 689-798, South Korea

³School of Chemical Engineering, Sungkyunkwan University, Suwon 300, South Korea

(Received 6 November 2013; accepted 28 November 2013; published online 26 December 2013)

Using the first-principles calculations, we explored the feasibility of using graphdiyne, a 2D layer of sp and sp^2 hybrid carbon networks, as lithium ion battery anodes. We found that the composite of the Li-intercalated multilayer α -graphdiyne was $C_6Li_{7.31}$ and that the calculated voltage was suitable for the anode. The practical specific/volumetric capacities can reach up to $2719 \text{ mAh g}^{-1}/2032 \text{ mAh cm}^{-3}$, much greater than the values of $\sim 372 \text{ mAh g}^{-1}/\sim 818 \text{ mAh cm}^{-3}$, $\sim 1117 \text{ mAh g}^{-1}/\sim 1589 \text{ mAh cm}^{-3}$, and $\sim 744 \text{ mAh g}^{-1}$ for graphite, graphynes, and γ -graphdiyne, respectively. Our calculations suggest that multilayer α -graphdiyne can serve as a promising high-capacity lithium ion battery anode. © 2013 AIP Publishing LLC.

[<http://dx.doi.org/10.1063/1.4850236>]

Lithium ion batteries are currently used in various portable electronics and are expected to be used in electric vehicles because it has a higher energy density than other rechargeable batteries. In these cases, bulk lithium metal was used as the anode. However, lithium metal anodes have some stability issues such as dendrite formation.^{1,2} Graphite has been shown to have high stability as an anode material because of its layered structure leading to high diffusivity of lithium ions and high stability through lithium intercalation. The maximum composite of Li-intercalated graphite is known to be C_6Li ,^{3–5} corresponding to the specific and the volumetric capacities as large as of 372 mAh g^{-1} and 818 mAh cm^{-3} , respectively. However, the search for new anode materials that have higher capacity has continued. The following minimum requirements must be met in order to qualify as an anode material: (i) the open circuit voltage (OCV) of the battery should be in the range of $\sim 0\text{--}2 \text{ V}$ when bulk Li is used as a reference electrode,² (ii) the specific (volumetric) capacity should be larger than that of graphite, 372 mAh g^{-1} (818 mAh cm^{-3}),² (iii) the volume expansion from lithium insertion should be as small as that for graphite. However, segregation of lithium takes place if the voltage is negative, and a candidate anode material will no longer work (though such a material may work as a cathode) if the voltage is greater than $\sim 2 \text{ V}$.

Recently, it has been reported that graphynes, 2D atomic layers consisting of two adjacent sp -bonded carbon atoms and sp^2 -bonded carbon atoms, exhibit intriguing electronic properties such as symmetric as well as asymmetric Dirac cones.^{6–10} Another attractive feature is that the surface area of graphyne is larger than that of graphene because its hexagonal area is much larger. From an application point of view, the structural properties of graphyne could allow a variety of potential applications for energy storage. For instance, it has been found that calcium-decorated carbon chain networks

and calcium/lithium-decorated graphynes can be used as high-capacity hydrogen storage material due to the large surface area.^{11–14} Higher Li gravimetric density than the sp^2 -bonded carbon network is possible due to a larger number of Li adsorption sites. In fact, recent theoretical studies^{15,16} showed significant increases in both specific and volumetric capacity of Li-intercalated multilayer α - and γ -graphynes have been found; a specific capacity of 1117 mAh g^{-1} (three times that of graphite) and the volumetric capacity of 1364 and 1589 mAh cm^{-3} (cf. $\sim 818 \text{ mAh cm}^{-3}$ for graphite) have been suggested.¹⁶ While a bottom-up approach^{17,18} was proposed to synthesize sp - sp^2 carbon networks such as graphynes, graphdiyne, which is a 2D atomic layer consisting of four adjacent sp -bonded carbon atoms and sp^2 -bonded carbon atoms, was synthesized in the form of films.¹⁹ Some experiments show that new carbon allotropes of sp - sp^2 hybrid carbon networks could be synthesized in the immediate future. Since graphdiyne has more sp -bonded-carbon atoms than graphyne, graphdiyne has larger surface area than graphyne. Therefore, higher Li capacity is expected for graphdiyne than for graphyne.

Recently, Sun *et al.*²⁰ explored possible applications of a single-layer γ -graphdiyne for lithium storage by using the density-functional calculations. They found high Li mobility in multilayer γ -graphdiyne and Li intercalation density as high as C_6Li_2 . α -graphdiyne is a different graphdiyne with a honeycomb lattice like graphene, so its surface area for intercalation of lithium ions may be the largest because its surface area larger than that of other types of graphdienes. On the other hand, since α -graphdiyne is metallic while γ -graphdiyne is semiconducting with the density functional theory (DFT) bandgap of 0.53 eV ,^{21,22} α -graphdiyne would be advantageous in terms of the electronic conductivity requirement for anodes. In this study, we explored the feasibility of monolayer or multilayer α -graphdiyne for lithium ion battery anodes because the different symmetries and local geometries could lead to different lithium intercalation. We found that the voltage is suitable for the anodes and

^{a)}Author to whom correspondence should be addressed. Electronic mail: hkiee3@konkuk.ac.kr

the maximum composite of Li-intercalated multilayer α -graphdiyne is $C_6Li_{7.31}$. This corresponds to specific/volumetric capacities of $2719\text{ mAh g}^{-1}/2032\text{ mAh cm}^{-3}$, much greater than the values of $\sim 372\text{ mAh g}^{-1}/\sim 818\text{ mAh cm}^{-3}$, $\sim 1117\text{ mAh g}^{-1}/\sim 1589\text{ mAh cm}^{-3}$, and $\sim 744\text{ mAh g}^{-1}$ of graphite,¹ graphynes,¹⁶ and γ -graphdiyne,²⁰ respectively. Our calculations suggest that multilayer α -graphdiyne can serve as high-capacity lithium ion battery anodes.

Our calculations were performed using a first-principles method based on density functional theory²³ as implemented in the Vienna *Ab-initio* Simulation Package (VASP) with a projector-augmented-wave (PAW) method.²⁴ The exchange correlation energy functional was used with the generalized gradient approximation (GGA) in the Perdew–Burke–Ernzerhof scheme,²⁵ and the kinetic energy cutoff was set at 400 eV. Our model α -graphdiyne system was a 1×1 hexagonal cell containing 14 C atoms. A geometrical optimization of Li-adsorbed α -graphdiyne was carried out within a fixed 1×1 cell obtained from the equilibrium lattice constant of the isolated graphdiyne until the Hellmann–Feynman force acting on each atom was less than 0.01 eV/\AA . The first Brillouin zone integration was done using the Monkhorst–Pack scheme.²⁶ A $4 \times 4 \times 1$ k -point sampling was done for the 1×1 α -graphdiyne. To remove spurious interactions between image structures due to periodic calculations, a vacuum layer of 12 \AA was taken in each of all nonperiodic directions. For Li-intercalated AB stacking multilayer, α -graphdiyne with a $1 \times 1 \times 2$ supercell was considered with the $4 \times 4 \times 2$ k -point sampling. Multilayer graphdiyne calculations were done with the GGA-D2 method,²⁷ which describes the interlayer van der Waals interaction including the attractive part of Lenard-Johns potential.

To explore the applications of α -graphdiyne as anodes, we performed calculations on Li adsorption on α -graphdiyne, a honeycomb lattice consisting of adjacent-four- sp -bonded carbon chains and sp^2 -bonded carbon atoms as shown in Figure 1. We performed calculations on Li adsorption on four

local geometries of Li atoms, on top of sp -bonded carbon atoms, sp^2 -bonded carbon atoms, and on the bonds between sp -bonded carbon atoms and sp^2 -bonded carbon atoms or between the sp -bonded carbon atoms: Li adsorption depends only on the local geometries such as on top of atoms or bonds. We found three adsorption configurations as shown in Figure 1(a), and out-of-plane adsorption of Li atoms on the edge of the hexagon is found to be of the lowest energy configuration when each hexagon accommodates one Li atom. Unlike multilayer γ -graphdiyne that Li atoms are attached with the in-plane configuration,²⁰ when one Li atom is added further, out-of-plane adsorption of Li atoms gets in to favorable energy as shown in Figure 1(b). The binding energy of Li atoms on a 1×1 α -graphdiyne was calculated as a function of the Li concentration x , where x is defined in C_6Li_x . Here, the binding energy of Li atoms is defined by $E_{bind}^x(Li) = (E_C + N \cdot E_{Li} - E_{C-Li}^x)/N$, where N is the number of Li atoms attached per 1×1 cell for a given x , E_{C-Li}^x is the total energy of Li-dispersed in a 1×1 graphdiyne with a x concentration of Li atoms, E_C is the total energy of an 1×1 isolated α -graphdiyne, and E_{Li} is the total energy of an isolated Li atom in a vacuum.

The composites of Li-dispersed α -graphdiyne shown in Figure 1 are (a) $C_6Li_{0.43}$ and (b) $C_6Li_{0.86}$, respectively. Three adsorption geometries at the composite of $C_6Li_{0.43}$ are shown in Figure 1(a) when each hexagon accommodates one Li atom. The most favorable adsorption site is out-of-plane and slightly off center of the edge of the hexagon, as shown in Figure 1(a), where the distance between the Li atom and the nearest C atom is $\sim 2.12\text{ \AA}$ and the Li binding energy is $\sim 1.88\text{ eV/Li}$. At higher concentration, the favorable site is out-of-plane and slightly off center of the edge as shown in Figure 1(b) when each hexagon accommodates two Li atoms. This is consistent with lower concentration case. The Li binding energies on α -graphdiyne are greater than the cohesive energy ($\sim 1.6\text{ eV}$) of bulk Li.¹⁶ From this, we expect

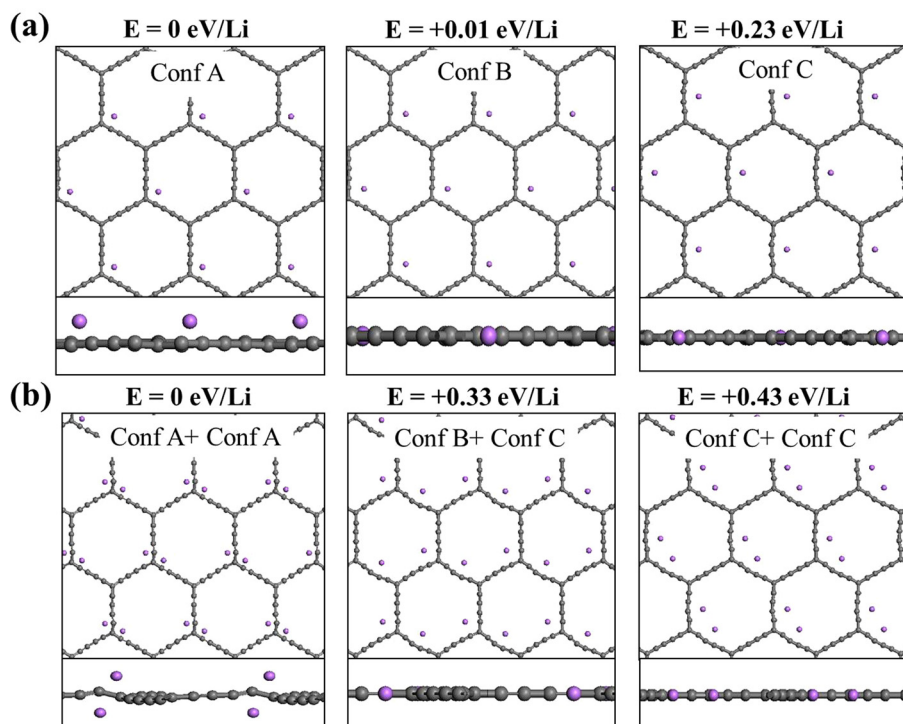


FIG. 1. Cross section view and side view for three different atomic structures of Li atoms attached on single layer α -graphdiyne at the (a) $x=0.43$ and (b) $x=0.86$ concentrations. The grey and purple dots represent carbon atoms and lithium atoms, respectively. The total energy E for the geometries is presented, where the energy for the lowest configuration is set to zero.

that Li atoms can be dispersed on α -graphdiyne without segregation of Li. The calculated binding energies of Li atoms on the graphdiyne are smaller than the corresponding GGA values of 2.21 eV/Li (2.69 eV/Li) on α -(γ -)graphyne, but larger than 1.10 eV/Li on graphene,²⁸ 1.80 eV/Li on a C₆₀,²⁹ and 0.34 (0.41) eV/Li on the inner (outer) shell of a (5,5) carbon nanotube.³⁰ The value is comparable to 1.83 eV/Li on carbyne.³¹ The binding energy of Li atoms may be increased by enhancing the electrostatic interaction between the Li+ atom and the C- atom due to their reduced dimensionality compared to other materials.

We carried out calculations on the adsorption of Li atoms on the graphdiyne as the concentration x increases. When four Li atoms are placed on each hexagon, two Li atoms are attached with an in-plane configuration and the other Li atoms undergo out-of-plane adsorption (Figure 2(a)). In general, out-of-plane adsorption of Li atoms is preferred as the concentration becomes higher. We also found that the sp-bonded carbon atoms are distorted by Li adsorption like a zigzag carbon chain and each sp-bonded carbon atom adsorbs two Li atoms as shown in Figure 2(d). This is similar to the geometry of Li adsorption to carbyne,³¹

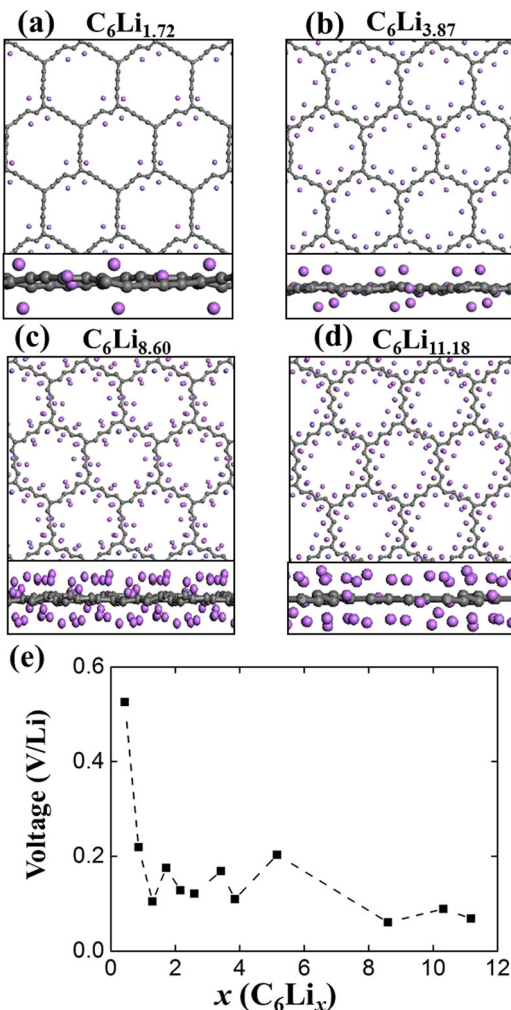


FIG. 2. The cross section view and side view for the optimized atomic structures of Li attached to single-layer α -graphdiyne at the different concentrations, (a) C₆Li_{1.72}, (b) C₆Li_{3.87}, (c) C₆Li_{8.60}, and (d) C₆Li_{11.18}. (e) The calculated average voltage per Li atom as a function of the concentration x .

but is in contrast to Li adsorption on α -graphyne where Li atoms are attached to in-plane hexagons with some distortion along the in-plane direction. To investigate the usability of Li-dispersed α -graphdiyne for anodes, the open circuit voltage (V_{OCV}) is calculated as a function of x

$$V_{OCV}(x) = \frac{E_C + N \cdot E_{Li}^{bulk} - E_{C-Li}^x}{eN}, \quad (1)$$

where e is the charge of electron and E_{Li}^{bulk} is the total energy per Li of bcc lithium. As shown in Figure 2(e), V_{OCV} decreases from ~ 0.5 V to ~ 0.1 V as the concentration increases as shown in Figure 2(e), which is due to the stronger Li-Li repulsive interaction at higher concentrations. The calculated V_{OCV} is in the window of the required voltage for anodes. Since the added voltage is negative when the concentration is over ~ 11.20 , we set the maximum composite of the Li-dispersed graphdiyne may be expected to be C₆Li_{11.18}, corresponding to the specific capacity of 4259 mAh g⁻¹. This is comparable to the value ~ 4800 mAh g⁻¹ of Li-dispersed carbyne.³¹ This result shows that as far as the Li adsorption is concerned, α -graphdiyne acts as a two-dimensional carbon chain network.

A layered structure such as graphite is desirable for anode materials because of the diffusivity of Li, the small volume change through Li intercalation between the layers, long life cycle by good reversibility of Li insertion and extraction, and good scalability. So, multilayer graphdinyes could be a possible replacement for lithium ion battery anodes. Since AB stacking multilayer α -graphdiyne is energetically favorable, we performed calculations on Li intercalation to AB stacking multilayer α -graphdiyne. From the calculations of Li dispersion on single-layer α -graphdiyne discussed above, we predicted stable Li-intercalated multilayered α -graphdiyne structures. Figure 3 shows the optimized geometries of Li-intercalated multilayer α -graphdiyne along with the voltage of Li atoms for different concentrations of x with different interlayer distance from 2.75 Å to 3.75 Å. The lowest energy interlayer distance was found to be 3.25 Å near high Li concentrations as shown in Figure 3(a). Figure 4 shows the cross section and side views, respectively, of Li-intercalated AB stacking α -graphdiyne with different concentrations where the layer-to-layer distance is 3.25 Å. The Li atoms are intercalated between the layers, and the local geometry of the adsorbed Li atoms is similar to that in Li-dispersed carbyne.³¹ The computed equilibrium layer-to-layer distance of the AB-stacked α -graphdiyne estimated with the GGA-D2 calculation is 3.15 Å. Therefore, as a result of the Li intercalation, the interlayer distance increases from 3.15 Å to 3.25 Å, while the lattice constant along with the in-plane direction is unchanged. This corresponds to the volume expansion of $\sim 3\%$, which is smaller than that of $\sim 12\%$ of Li-intercalated graphite where the interlayer distance increases from 3.35 Å to 3.76 Å.³² So, the requirement of the volume change by Li intercalation is met.

Since the OCV on multilayer α -graphdiyne is positive in the concentration range as shown in Figure 3(b), it is concluded that Li atoms are intercalated without segregation within the range. However, we chose $x = 7.31$ for the maximum Li concentration because the further intercalation process is endothermic. Therefore, the maximum configuration

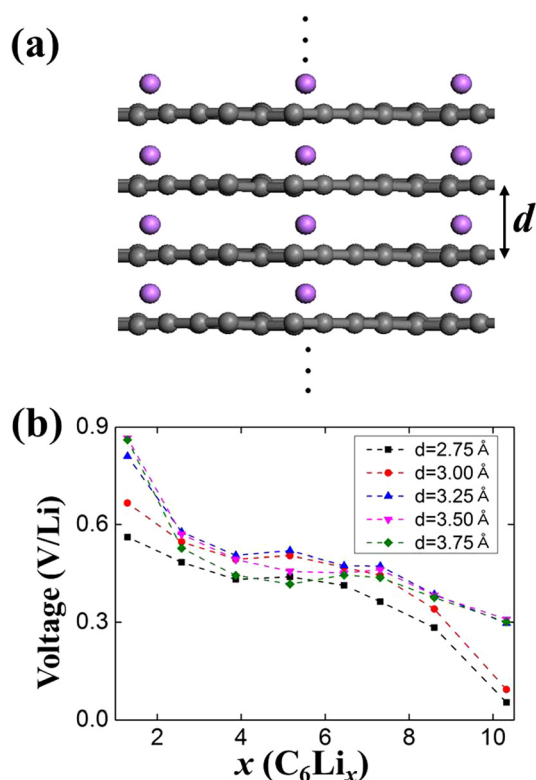


FIG. 3. (a) Schematic of Li-intercalated AB-stacking multilayer α -graphdiyne as different interlayer instances. (b) The calculated average voltage per Li for Li atoms intercalated to the AB-stacking multilayer α -graphdiyne as a function of the concentration, x .

expected for Li-intercalated multilayer α -graphdiyne is $C_6Li_{7.31}$. This composite corresponds to the practical specific capacity of 2719 mAh g^{-1} , which is significantly greater than 372 mAh g^{-1} and 1117 mAh g^{-1} of Li-intercalated graphite and multilayer graphynes with the composite of C_6Li_3 , respectively.¹⁶ In addition, the calculated practical volumetric capacity of Li-intercalated multilayer α -graphdiyne ($C_6Li_{7.31}$) is 2032 mAh cm^{-3} , which is much greater than the capacity of graphite ($\sim 818 \text{ mAh cm}^{-3}$)¹ and multilayer graphynes (1364 mAh cm^{-3} and 1589 mAh cm^{-3} for α - and γ -graphynes with the composite of C_6Li_3).¹⁶ The results suggest that multilayer α -graphdiyne can serve as high-capacity anode materials.

We have investigated energetics and geometry optimization of Li-dispersed monolayer and Li-intercalated AB-stacked multilayer α -graphdiyne as a promising anode material. The sp-bonded carbon atoms of α -graphdiyne bind Li atoms resulting in a desirable voltage for anodes and the local adsorption geometry, i.e., a zigzag chain, is similar to that of a one-dimensional carbon chain of carbyne. Four-adjacent-sp-bonded carbon chain is the minimum length mimicking carbyne. Since Li adsorption geometries are similar to those of carbyne, the Li capacity of multilayer α -graphdiyne may be highest among 2D layers of sp-sp² hybrid carbon networks or when compared to other carbon nanostructures consisting of sp²-bonded carbon atoms. This means that α -graphdiyne acts like a 2D carbon chain. The volumetric capacity of 2D sp-sp² hybrid networks is significantly reduced as the length of the sp-bonded carbon chains increases. Thus, α -graphdiyne is an optimal candidate for lithium ion anodes when both specific and volumetric

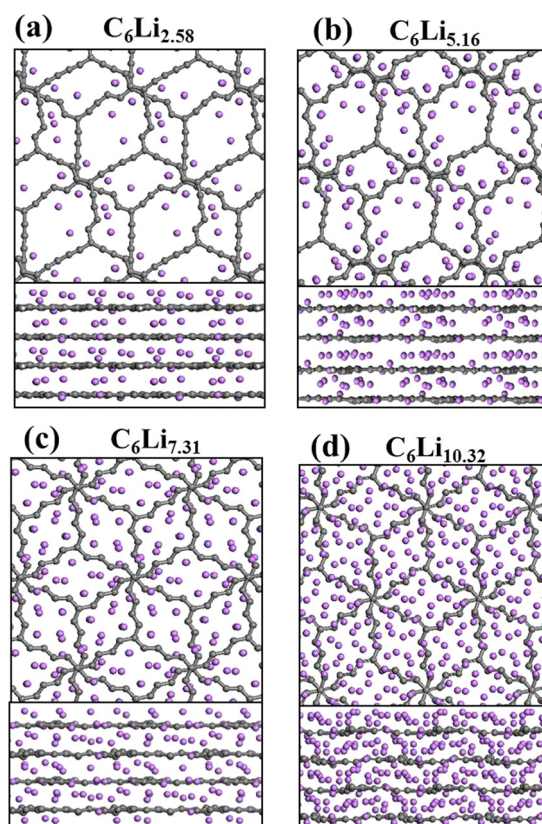


FIG. 4. The cross section view and side view for the optimized atomic structures of Li-intercalated AB-stacking multilayer α -graphdiyne with the different concentrations, (a) $C_6Li_{2.58}$, (b) $C_6Li_{5.16}$, (c) $C_6Li_{7.31}$, and (d) $C_6Li_{10.32}$.

capacities are considered. We note that the structural stability of α -graphdiyne in the process of Li intercalation/deintercalation is critical for their practical implementations as anodes, especially considering that the calculated cohesive energies of α - and γ -graphdienes (7.0 eV and 7.2 eV, respectively) or γ -graphyne (7.3 eV), are smaller than that of graphite ($\sim 8.0 \text{ eV}$). These values show the possibility that phase change from graphdiyne to graphite might occur during Li intercalation and deintercalation. Thus, an independent study on the stability during the electrochemical reaction will be necessary to verify them for the anode applications.

In conclusion, we performed total energy electronic structure calculations on Li-intercalated multilayer graphdienes, using first-principles density-functional theory, to explore their applicability as lithium ion battery anodes. The calculated voltage was found to be in a desirable voltage range of the anodes. The practical specific and volumetric Li capacity of multilayer α -graphdiyne can reach up to $\sim 2700 \text{ mAh g}^{-1}$ and $\sim 2000 \text{ mAh cm}^{-3}$, respectively, which is much larger than the values of $\sim 372 \text{ mAh g}^{-1}$ and $\sim 820 \text{ mAh cm}^{-3}$ of graphite. In addition, α -graphdiyne would be advantageous over other 2D layers of sp-sp² hybrid carbon networks because the volume change is negligible through Li intercalation. These results suggest that multilayer α -graphdiyne has considerable potential as a promising high-capacity lithium ion battery anode material.

This work was supported by the Basic Science Research Program (Grant No. KRF-2012R1A1A1013124 and Grant No. 2012R1A1A2043431) through the National Research

Foundation of Korea, funded by the Ministry of Education, Science and Technology. The authors also acknowledge support from KISTI under the Supercomputing Applications Support Program (KSC-2013-C3-025).

- ¹E. Stura and C. Nicolini, *Anal. Chim. Acta* **568**, 57 (2006).
- ²B. J. Landi, M. J. Ganter, C. D. Cress, R. A. DiLeo, and R. P. Raffaele, *Energy Environ. Sci.* **2**, 638 (2009).
- ³J. R. Dahn, *Phys. Rev. B* **44**, 9170 (1991).
- ⁴A. Satoh, N. Takami, and T. Ohsaki, *Solid State Ionics* **80**, 291 (1995).
- ⁵M. Balasubramanian, C. S. Johnson, J. O. Cross, G. T. Seidler, T. T. Fister, E. A. Stern, C. Hammer, and S. O. Mariager, *Appl. Phys. Lett.* **91**, 031904 (2007).
- ⁶O. Leenaerts, B. Partoens, and F. M. Peeters, *Appl. Phys. Lett.* **103**, 013105 (2013).
- ⁷Y. Y. Zhang, Q. X. Pei, and C. M. Wang, *Appl. Phys. Lett.* **101**, 081909 (2012).
- ⁸D. Malko, C. Neiss, F. Vines, and A. Gorling, *Phys. Rev. Lett.* **108**, 086804 (2012).
- ⁹B. G. Kim and H. J. Choi, *Phys. Rev. B* **86**, 115435 (2012).
- ¹⁰J. Chen, J. Xi, D. Wang, and Z. Shuai, *J. Phys. Chem. Lett.* **4**, 1443 (2013).
- ¹¹H. J. Hwang, Y. Kwon, and H. Lee, *J. Phys. Chem. C* **116**, 20220 (2012).
- ¹²Y. Guo, K. Jiang, B. Xu, Y. Xia, J. Yin, and Z. Liu, *J. Phys. Chem. C* **116**, 13837 (2012).
- ¹³C. Li, J. Li, F. Wu, S.-S. Li, J.-B. Xia, and L.-W. Wang, *J. Phys. Chem. C* **115**, 23221 (2011).
- ¹⁴T. Hussain, B. Pathak, M. Ramzan, T. A. Maark, and R. Ahuja, *Appl. Phys. Lett.* **100**, 183902 (2012).
- ¹⁵H. Zhang, M. Zhao, X. He, Z. Wang, X. Zhang, and X. Liu, *J. Phys. Chem. C* **115**, 8845 (2011).
- ¹⁶H. J. Hwang, J. Koo, M. Park, N. Park, Y. Kwon, and H. Lee, *J. Phys. Chem. C* **117**, 6919–6923 (2013).
- ¹⁷J. M. Kehoe, J. H. Kiley, J. J. English, C. A. Johnson, R. C. Petersen, and M. M. Haley, *Org. Lett.* **2**, 969 (2000).
- ¹⁸C. A. Johnson II, Y. Lu, and M. M. Haley, *Org. Lett.* **9**, 3725 (2007).
- ¹⁹G. X. Li, Y. L. Li, H. B. Liu, Y. B. Guo, Y. J. Li, and D. B. Zhu, *Chem. Commun.* **46**, 3256 (2010).
- ²⁰C. Sun and D. J. Searles, *J. Phys. Chem. C* **116**, 26222 (2012).
- ²¹L. D. Pan, L. Z. Zhang, B. Q. Song, S. X. Du, and H.-J. Gao, *Appl. Phys. Lett.* **98**, 173102 (2011).
- ²²G. Luo, X. Qian, H. Liu, R. Qin, J. Zhou, L. Li, Z. Gao, E. Wang, W.-N. Mei, J. Lu, Y. Li, and S. Nagase, *Phys. Rev. B* **84**, 075439 (2011).
- ²³W. Kohn and L. J. Sham, *Phys. Rev.* **140**, A1133 (1965).
- ²⁴G. Kresse and D. Joubert, *Phys. Rev. B* **59**, 1758 (1999).
- ²⁵J. P. Perdew, K. Burke, and M. Ernzerhof, *Phys. Rev. Lett.* **77**, 3865 (1996).
- ²⁶H. J. Monkhorst and J. D. Pack, *Phys. Rev. B* **13**, 5188 (1976).
- ²⁷S. Grimme, *J. Comput. Chem.* **27**, 1787 (2006).
- ²⁸K. T. Chan, J. B. Neaton, and M. L. Cohen, *Phys. Rev. B* **77**, 235430 (2008).
- ²⁹Q. Sun, P. Jena, Q. Wang, and M. Marquez, *J. Am. Chem. Soc.* **128**, 9741 (2006).
- ³⁰Z. Zhou, X. Gao, J. Yan, D. Song, and M. Morinaga, *J. Phys. Chem. B* **108**, 9023 (2004).
- ³¹M. Park and H. Lee, *J. Korean Phys. Soc.* **63**, 1014 (2013).
- ³²K. Persson, Y. Hinuma, Y. S. Meng, A. V. d. Ven, and G. Ceder, *Phys. Rev. B* **82**, 125416 (2010).